Stress Analysis in Edentulous Mandibular Bone Supporting Implant-Retained 1-piece or Multiple Superstructures

Sawako Yokoyama, DDS[1]/Noriyuki Wakabayashi, DDS, PhD[2]/Makoto Shiota, DDS, PhD[3]/
Takashi Ohyama, DDS, PhD[4]

Purpose: *The aim of this study was to investigate the stress distribution in mandibular bone supporting a single or separate multiple implant-retained superstructures.* ***Materials and Methods:*** *Three-dimensional finite element models consisting of the mandibular bone, 8 implants, and 1 or more superstructures were created. Vertical and oblique loads were directed onto the occlusal areas of the superstructures to simulate the maximum intercuspal contacts and working contacts, such as the canine-protected and group function occlusion.* ***Results:*** *The unseparated 1-piece superstructure generated the lowest maximum equivalent stresses in the peri-implant bone, followed by the 2-piece superstructure separated at the midline. For the 3-piece superstructure, which was separated between the canine and the premolar, the maximum stress was lower when the canine on the working side was loaded than when the posterior teeth were loaded.* ***Discussion:*** *Separating the 1-piece superstructure into 2- to 4-piece superstructures increased the mechanical stress around supporting implants. Canine load on the working side is distributed well in 1-piece and 3-piece superstructures.* ***Conclusion:*** *Based on the results of this finite element model study, canine protected occlusion is recommended for 1-piece and 3-piece superstructures. The unseparated superstructure was more effective in relieving stress concentration in the edentulous mandibular bone than the separated superstructures.* INT J ORAL MAXILLOFAC IMPLANTS 2005;20:578–583

Key words: *bone, dental implants, finite element analysis, implant-supported superstructure, stress*

The use of osseointegrated implants as abutments for fixed complete dentures (FCDs) is a prospective treatment procedure designed to improve the masticatory function of completely edentulous patients, especially for those who are dissatisfied with their removable dentures.[1–4] FCDs have mostly been produced as 1-piece superstructures with distal cantilevers supported by anterior implants. Even though the applicability of implants placed in the molar region has increased by virtue of innovative materials and techniques, including shorter implants, bone grafts, and lateralization of the alveolar nerve,[5–8] 1-piece superstructures remain the first choice when designing implant-retained prostheses.

On the other hand, in long-term maintenance, it is essential to manage the possible risks of mechanical or biologic problems in a few among several implants, or local failures in long-span superstructures. Lekholm and associates[9] reported that after 10 years of clinical follow-up, the cumulative survival rate for original prostheses was 86.5%, compared to the overall implant survival rate of 92.6%. A remake of the entire superstructure because of local failures may consume considerable amounts of both the patient's and the clinician's time, energy, and eco-

[1]Resident, Implantology, Department of Masticatory Function Rehabilitation, Division of Oral Health Sciences, Graduate School, Tokyo Medical and Dental University, Tokyo, Japan.
[2]Research Associate, Removable Prosthodontics, Department of Masticatory Function Rehabilitation, Division of Oral Health Sciences, Graduate School, Tokyo Medical and Dental University, Tokyo, Japan.
[3]Associate Professor, Implantology, Department of Masticatory Function Rehabilitation, Division of Oral Health Sciences, Graduate School, Tokyo Medical and Dental University, Tokyo, Japan.
[4]Professor and Chair, Removable Prosthodontics, Department of Masticatory Function Rehabilitation, Division of Oral Health Sciences, Graduate School, Tokyo Medical and Dental University, Tokyo, Japan.

Correspondence to: Dr Sawako Yokoyama, 1-5-45 Yushima, Bunkyo, Tokyo 113-8549, Japan. Fax: +81 3 5803 5842. E-mail: sawako.impl@tmd.ac.jp

This material was presented at the 12th Annual Scientific Congress of the European Association for Osseointegration, Vienna, Austria, October 2003.

nomic resources. Multiple superstructures or fixed partial dentures (FPDs) allow the damaged part of the prosthesis to be replaced while the undamaged parts are retained, minimizing the costs of repair.

Separating the superstructure into small pieces has reportedly had some negative effects on stress concentrations around implants in the bone.[10,11] However, these study designs were limited to unilateral short-span superstructures and parts of the mandible supporting a small number of implants. An excessive stress concentration might facilitate bone resorption under the functional occlusal loadings, thus compromising the longevity of the implants.[12–14] The effects of separating FCDs into multiple FPDs on the whole mandibular bone have not been sufficiently assessed in relation to the site and the direction of the occlusal loadings.

The purpose of this study was to investigate the effects of separating a 1-piece, implant-supported superstructure into multiple FPDs on stress distributions in the edentulous mandibular bone under simulated occlusal loadings. In addition, the optimal working side contact scheme for suppression of the maximum stress in the bone with reference to the site of the separation was assessed.

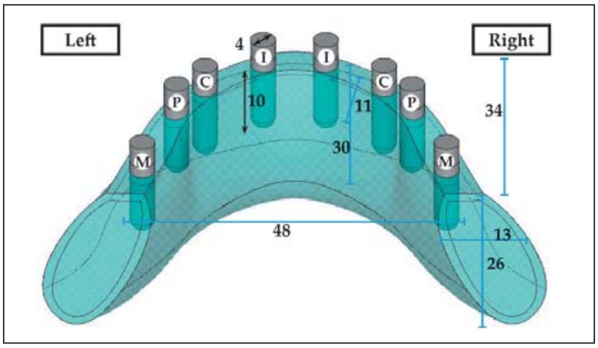

Fig 1a The finite element model of the mandibular bone and the implants with their dimensions in millimeters. The capital letters indicate the locations of the implants (I = central incisor, C = canine, P = first premolar, M = first molar).

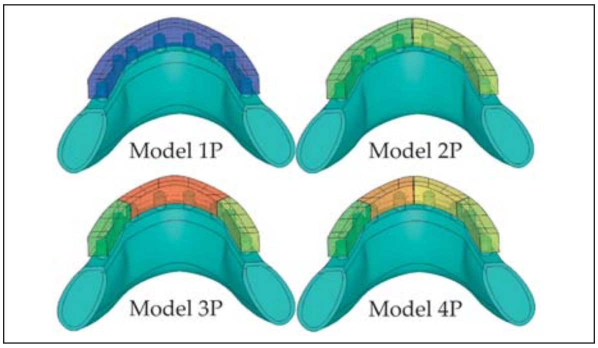

Fig 1b The superstructures used in the models. Model 1P was the 1-piece superstructure (the blue rim in Model 1P); the 2-piece superstructures separated between the central incisors (light and dark green rims in Model 2P); the 3-piece superstructures separated between the canine and the first premolar on both sides (red, light green, and dark green rims in Model 3P); and the 4-piece superstructures separated between the central incisors and between the canines and the first premolars (light green, dark green, orange, and yellow rims in Model 4P).

MATERIALS AND METHODS

Finite Element Models

Four 3-dimensional finite element models were created (Ansys 7.0, Ansys, Canonsburg, PA) in this study. Each model consisted of the mandibular bone, 8 osseointegrated implants, abutments, and 1 of 4 superstructures (Figs 1a and 1b). The bone was modeled as a cancellous core surrounded by a 1.5-mm-thick cortical bone. The widths of the mandible on the horizontal plane at the upper one-third and two-thirds levels were 11.0 mm and 11.5 mm at the incisor region, 11.0 mm and 14.0 mm at the canine region, 11.0 mm and 11.5 mm at the first premolar region, and 13.0 mm and 14.0 mm at the second molar region, respectively. The heights of the mandible at the same regions were 30 mm, 30 mm, 28 mm, and 26 mm, respectively. In each model, cylinders 4 mm in diameter and 10 mm in length were embedded as dental implants at the missing central incisor (I), canine (C), first premolar (P), and first molar (M) locations on both sides of the arch.

The 1-piece horseshoe rim was 8 mm in height and 5 mm (anterior region) to 6 mm (posterior region) in width. This was assumed to be a superstructure in the form of a FCD and was used in Model 1P. The 2-piece superstructure was created by separating the FCD at the midline (Model 2P). The 3-piece superstructure was made by separating the FCD between the canine and the premolar on both sides (Model 3P). The 4-piece superstructure was constructed by separating the FCD at the midline and between the canines and premolars (Model 4P). It was assumed that each superstructure did not mechanically affect the others at the proximal contacts.

Material Properties and Meshing

All materials were considered to be homogeneous, isotropic, and linearly elastic. Poisson's ratio (ν) and Young's modulus (E) were 0.3 and 14.7 GPa for the cortical bone, 0.3 and 0.49 GPa for the cancellous bone, and 0.33 and 117 GPa for the implants and the FCDs, respectively.[15–17] The interfaces between the materials were assumed to be bonded or osseointegrated. Each model was meshed by elements determined by 8 nodes in the tetrahedral bodies. Each model consisted of approximately 71,500 elements and 16,700 nodes (Fig 2).

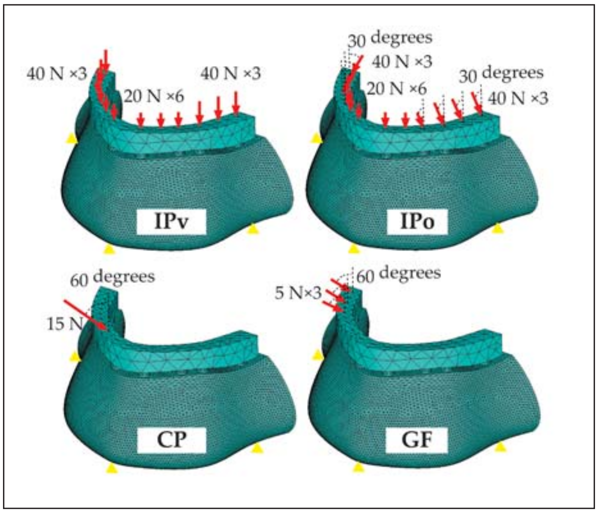

Fig 2 The meshed model with the loading and boundary conditions. The red arrows indicate the vertical and off-axis oblique loads on the occlusal surface of each artificial tooth position. For the IPv and IPo conditions, each red arrow indicates a load of 20 N (anterior region) or 40 N (posterior region) on an individual tooth location. A red arrow indicates a load of 15 N on the right canine for the CP, and a load of 5 N on each of the 3 right posterior teeth in the GF. The yellow triangles represent the fixation at the inferior surface of the mandible.

Loading and Boundary Conditions

Static loads were applied on the occlusal surfaces of selected teeth positions. These positions were located in the occlusal rims and were assumed to be opposing a fully dentate or fully restored maxilla. As with the maximum intercuspal contacts, 2 loading conditions were simulated (simulations IPv and IPo). In simulation IPv, a vertical load of 20 N was simultaneously directed on an occlusal area of each of the central incisors, lateral incisors, and canines, and a vertical load of 40 N was directed on each of the first and second premolars and the first molars. In simulation IPo, a vertical load of 20 N was directed on the incisors, and an oblique load of 20 N for each canine and 40 N for each premolar and first molar were directed 30 degrees buccal from the vertical. These loads were based on a previous study that reported the maximum bite forces of subjects with fixed cross-arch prostheses in natural dentition.[18]

Two patterns of working side contacts in the lateral excursion of the mandible were simulated. In the canine protected occlusion simulation (simulation CP), an oblique load of 15 N was loaded on the right canine 60 degrees lingual from the vertical. In the group function occlusion simulation (simulation GF), an oblique load of 5 N was loaded simultaneously on each of the right premolars and the first molar (total 15 N) in the same direction as simulation CP (Fig 2).

No displacement of the outer surface of the lower third of the mandibular bone was prescribed to simulate the support of the masseter and medial pterygoid muscles that attach to the outside and inside of the mandible angle. The von Mises' equivalent stress distributions in the bone were calculated for all the models under all of the loading conditions.

RESULTS

Simulation IPv

In all of the loading conditions, there were no noticeable differences in the stress distributions among the models (Figs 3a and 3b). In the cortical bone, the highest maximum equivalent stresses were observed around the implant at the first molar location (approximately 4.0 MPa). The lowest maximum stresses were detected around the incisor implants (1.0 MPa). The maximum stresses in the cancellous bone were observed in the apical region of the implants. The stresses were considerably lower than those in the cortical bone, with the highest value being 0.5 MPa in the model 4P at the first molar implant.

Simulation IPo

Similar to simulation IPv, the highest maximum stresses in the bone in simulation IPo were observed in the cervical region at the molar implants (Figs 4a and 4b). However, there were clear differences in the stress among the models. The maximum stresses were lowest for model 1P for all locations. The highest maximum stress was recorded in the region adjacent to the molar implant in model 4P (13.8 MPa). In Model 2P, the stress was relatively insensitive to the implant location. The largest differences in stress were found among the implants in Model 3P, where the highest stress at the molar location (12.4 MPa) was approximately 6 times greater than that at the incisor location (1.9 MPa).

Simulation GF and CP

Model 1P demonstrated the lowest maximum stress among the models. The highest maximum stress value noted for this model was 1.3 MPa in the lingual cervical region of the right molar during simulation GF. In model 2P, the maximum stresses were highest at the right incisor during simulations CP and GF (1.8 MPa and 1.4 MPa, respectively), while the other implants on the right side indicated a relatively equal stress levels of approximately 1.0 MPa. In model 3P, the highest maximum stress was observed in the right premolar vicinity under simulation GF (2.8 GPa, 2.0 GPa in the right canine vicinity under simulation CP). In model 4P, slightly higher maximum stress was observed in the right canine vicinity under simula-

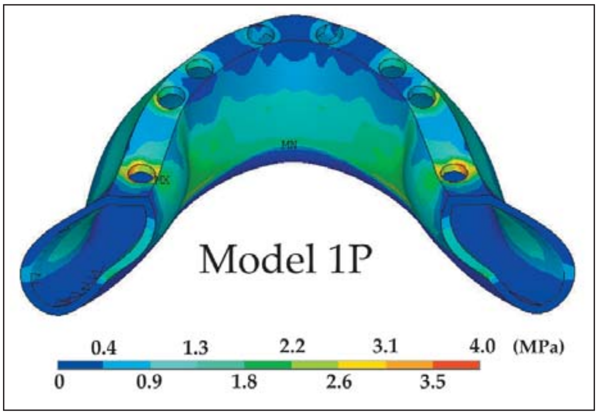

Fig 3a The contour graphic indicates the equivalent stress distribution in the cortical bone of model 1P under simulation IPv. The places where the stress was at its maximum (MX) and minimum (MN) are indicated.

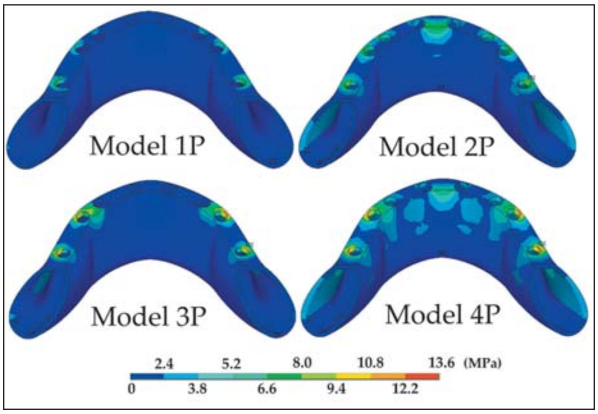

Fig 4a The contour graphics indicate the equivalent stress distributions in the cortical bone for all the models under simulation IPo.

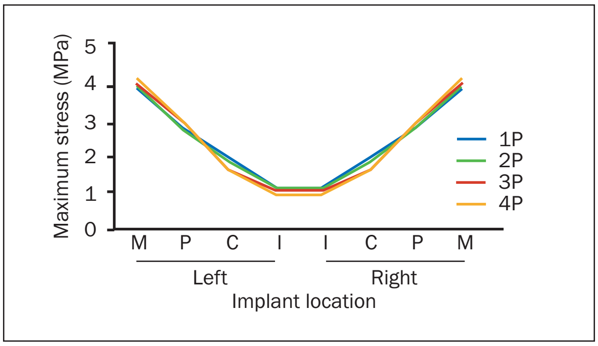

Fig 3b The maximum equivalent stresses in the cortical bone around the implants for all the models under simulation IPv. M = molar; P = premolar; C = canine; I = incisor.

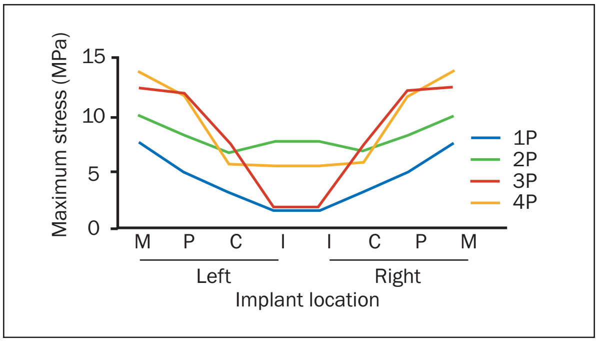

Fig 4b The maximum equivalent stresses in the cortical bone around the implants for all the models under simulation IPo.

tion CP (2.8 GPa) than in the right premolar vicinity under simulation GF (2.4 GPa) (Figs 5a and 5b).

In the cancellous bone, maximum stress data were excluded from the graphs because they were considerably lower than the data registered in the cortical bone in all the models under all the loading simulations.

DISCUSSION

The results of this study indicated that the use of a 1-piece FCD was effective in suppressing stress in the bone when it was subjected to oblique occlusal loads. These results are partially in agreement with a previous study[10] in which stresses in a small segment of the mandibular bone with 2 crowns and 2 implants were analyzed. The results of that study indicated that splinted FPDs generated approximately half of the maximum stress of the separated superstructures. The relatively low maximum stress recorded in the 1-piece FCD in the present study might be attributed to the superior load transferring ability of the structure. It is speculated that in the IPo condition, a horizontal component of the load, which could potentially induce harmful stress in the bone,[19,20] was offset by loads on the other locations in the broad 1-piece superstructure. However, a similar amount of compensation could not be expected in the separated superstructures.

In the cancellous bone, maximum equivalent stress was shown near the apical region of the implants. Significantly lower stresses were observed in the cancellous bone than in the cortical bone. This might be the result of the stress-transferring mechanism that occurred in the implant-bone complex. It is possible that the stresses induced by the occlusal loads are initially transferred from the implant to the cervical bone, while the small amount of remaining stress is spread to the cancellous bone at the apical region. It is also possible that higher stress values were observed in the cortical bone because cortical bone has a higher modulus of elasticity compared to

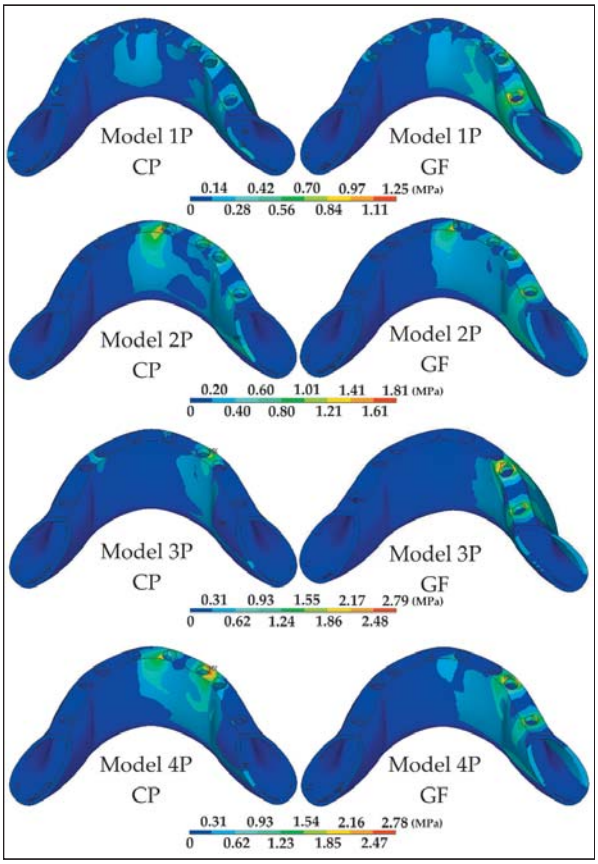

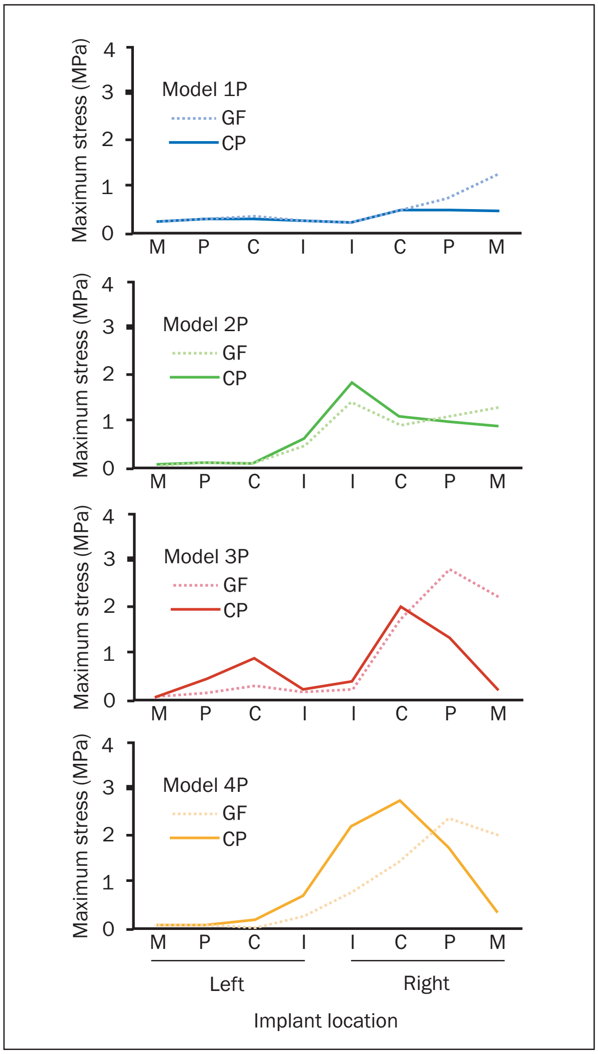

Fig 5a *(Above)* The contour graphics indicate the equivalent stress distributions in the cortical bone for all the models under simulations CP and GF.

Fig 5b *(Right)* The maximum equivalent stresses in the cortical bone around the implants for all the models under simulations CP and GF.

cancellous bone[21] and thus greater ability to transfer stress. The results of the present study corresponded to previous in vitro and in vivo studies[22–26] that have demonstrated bone loss is initiated in the region around the implant neck.

In regard to the working side contacts in the lateral excursion of the mandible, Wismeijer and associates[27] advocated that mandibular implant-retained FCDs should include group-function or mutually protected occlusion when the opposing maxilla was fully dentate. However, the results of this study indicated that the maximum stress generated by the 1-piece FCD was lower for the simulated canine-protected occlusion than for group-function occlusion. Since the bone model was wider in the posterior section than the anterior, it was assumed that the stress generated by the loads on the posterior teeth was well distributed and relieved by the larger volume of the bone, which then resulted in a lesser stress concentration. The conflicting results might be related to the fact that a single canine load was distributed well to the anterior and posterior implants nearby, while the posterior loads were predominantly supported by the posterior implants. It might also be related to the rigid structure of the anterior part of the bone, which has a U-shaped curvature in the midsection of the mandible.

In model 3P, in which the superstructure was separated between the canines and the premolars, the maximum stress was lower in simulation CP (2.0 MPa, at the canine implant) than in simulation GF (2.8 MPa, at the first premolar implant). This result may be explained by the fact that the anterior segment of the superstructure was supported by more implants ($n = 4$) than the posterior segment ($n = 2$). The rigid U-shaped alignment of the anterior implants might also have caused a reduction in the maximum stress induced by loading the canine. Considering the 3-piece superstructure, to avoid the potentially harmful stress peak in the posterior region of the bone, canine-protected occlusion for the working side contacts can be recommended. Model 2P, which was separated at the midline between the central incisors, demonstrated a relatively even stress distribution in the working side of the implant vicinity without any sensitivity to the working-side occlusal scheme. Because model 2P consists of unilateral superstructures supported by implants that are linearly arranged without the rigid U-shaped anterior alignment, a sufficient amount of anterior bone volume is desirable if the model 2P superstructure design is considered for use. When the superstructure was split at the sites between the canines and the premolars in addition to the midline separation (model 4P), a relatively high stress peak appeared in the canine implant under the CP, or at the posterior implants under the GF, which suggests a difficulty in the reduction of the maximum stress with this model.

CONCLUSIONS

According to this investigation, the 1-piece superstructure was more effective in relieving the stress concentration in the edentulous mandibular bone than were the separated superstructures. When planning to use a 1-piece FCD separated into 3 pieces as in the present study, canine-protected occlusion is recommended. The 2-piece superstructure separated at the midline created a relatively even stress distribution on the working side of the implant vicinity without a sensitivity to the working side occlusal scheme.

ACKNOWLEDGMENTS

This study was supported by Grants in Aid for Scientific Research, 12771170 (N.W.) and 14571840 (N.W.), from the Ministry of Education, Science, and Culture of Japan.

REFERENCES

1. Lindquist LW, Carlsson GE. Long-term effects on chewing with mandibular fixed prostheses on osseointegrated implants. Acta Odontol Scand 1985;43:39–45.
2. Carlsson GE, Lindquist LW. Ten-year longitudinal study of masticatory function in edentulous patients treated with fixed complete dentures on osseointegrated implants. Int J Prosthodont 1994;7:448–453.
3. Davis DM. Role of implants in the treatment of edentulous patients. Int J Prosthodont 1990;3:42–50.
4. Bergman B, Carlsson GE. Clinical long-term study of complete denture wearers. J Prosthet Dent 1985;53:56–61.
5. Lekholm U, Wannfors K, Isaksson S, Adielsson B. Oral implants in combination with bone grafts. A 3-year retrospective multicenter study using the Brånemark implant system. Int J Oral Maxillofac Surg 1999;3:181–187.
6. Cheung LK, Leung ACF. Dental implants in reconstructed jaws: Implant longevity and peri-implant tissue outcomes. Int J Oral Surg 2003;61:1263–1274.
7. Rosenquist B. Fixture placement posterior to the mental foramen with transpositioning of the inferior alveolar nerve. Int J Oral Maxillofac Implants 1992;1:45–50.
8. Peleg M, Mazor Z, Chaushu G, Garg AK. Lateralization of the inferior alveolar nerve with simultaneous implant placement: A modified technique. Int J Oral Maxillofac Implants 2002;17:101–106.
9. Lekholm U, Gunne J, Henry P, et al. Survival of the Brånemark implant in partially edentulous jaws: A 10-year prospective multicenter study. Int J Oral Maxillofac Implants 1999;5:639–645.
10. Wang TM, Leu LJ, Wang JS, Lin LD. Effects of prosthesis materials and prosthesis splinting on peri-implant bone stress around implants in poor-quality bone: A numeric analysis. Int J Oral Maxillofac Implants 2002;2:231–237.
11. Sato T, Kusakari H, Miyakawa O. Three dimensional finite element analysis of bone around dental implants in posterior mandibular region—Biomechanics of implant connections. J Jpn Prosthodont Soc 1996;40:682–694.
12. Brånemark P-I. Osseointegration and its experimental background. J Prosthet Dent 1983;50:399–410.
13. Isidor F. Loss of osseointegration caused by occlusal load of oral implants. A clinical and radiographic study in monkeys. Clin Oral Implants Res 1996;7:143–152.
14. Brunski JB. Biomechanical considerations in dental implant design. Int J Oral Implantol 1988;5:31–34.
15. Moroi HH, Okimoto K, Moroi R, Terada Y. Numeric approach to the biomechanical analysis of thermal effects in coated implants. Int J Prosthodont 1993;6:564–572.
16. Bever MB. Encyclopedia of Materials Science and Engineering. New York: Pergamon Press, 1986:1059.
17. Farah JW, Craig RG, Meroueh KA. Finite element analysis of three- and four-unit bridges. J Oral Rehabil 1989;16:603–611.
18. Lundgren D, Laurell L. Occlusal force pattern during chewing and biting in dentitions restored with fixed bridges of cross-arch extension: I. Bilateral end abutments. J Oral Rehabil 1986;13:57–71.
19. Richter EJ. In vivo horizontal bending moments on implants. Int J Oral Maxillofac Implants 1998;2:232–244.
20. Sahin S, Cehreli MC, Yalcin E. The influence of functional forces on the biomechanics of implant-supported prostheses—A review. J Dent 2002;30:271–282.
21. Chou PC, Pagano NJ. Elasticy: Tensor, Dyadic, and Engineering Approaches. New York: Dover Publications, 1992:55.
22. Adell R, Lekholm U, Rockler B, Brånemark P-I. A 15-year study of osseointegrated implants in the treatment of the edentulous jaw. Int Oral Surg 1981;10:387–416.
23. Lozada JL, Abbate MF, Pizzarello FA, James RA. Comparative three-dimensional analysis of two finite-element endosseous implant designs. J Oral Implantol 1994;20:315–321.
24. Morgan MJ, James DF, Pilliar RM. Fractures of the fixture component of an osseointegrated implant. Int J Oral Maxillofac Implants 1993;8:409–414.
25. Barbier L, Vander Sloten J, Krzesinski G, Schepers E, Van der Perre G. Finite element analysis of non-axial versus axial loading of oral implants in the mandible of the dog. J Oral Rehabil 1998;25:847–858.
26. Hoshaw SJ, Brunski JB, Cochran GVB. Mechanical loading of Brånemark implants affects interfacial bone modeling and remodeling. Int J Oral Maxillofac Implants 1994;9:345–359.
27. Wismeijer D, van Waas M, Kalk W. Factors to consider in selecting an occlusal concept for patients with implants in the edentulous mandible. J Prosthet Dent 1995;4:380–384.